

Electrical conductivity, TEP and dielectric studies on mol % 66.6 AgI-22.2 Ag₂O-11.1 (0.8 V₂O₅-0.2 P₂O₅) electrolyte material for solid state batteries

P. SATHYA SAINATH PRASAD, S. RADHAKRISHNA

Department of Physics, Indian Institute of Technology, Madras 600 036, India

In the superionic conducting quarternary system AgI-Ag₂O-V₂O₅-P₂O₅, the best ionic conductivity was obtained for the composition 66.6% AgI-33.3% (2Ag₂O-1 (V₂O₅-P₂O₅)), when the GF/GM ratio was varied from 0.20 to 5.0. Then fixing the GF/GM ratio at 0.50, the ratio of the glass formers V₂O₅ and P₂O₅ were varied and the highest conducting composition was obtained as 66.6% AgI-22.2 Ag₂O-11.1% (0.8 V₂O₅-0.2 P₂O₅). A preliminary investigation using this material in the form of an electrolyte in a solid state electrochemical cell is reported. The polycrystalline and amorphous compounds were prepared from the same melt, by open air crucible melting and the rapid quenching technique. The ionic conductivity for the best conducting polycrystalline (hence referred as 66VP82P) and amorphous (66VP82G) samples was obtained as 8.3×10^{-3} and $4.2 \times 10^{-2} \Omega^{-1} \text{ cm}^{-1}$ respectively. The electronic conductivity of the order $10^{-10} \Omega^{-1} \text{ cm}^{-1}$ was observed for 66VP82G and $10^{-8} \Omega^{-1} \text{ cm}^{-1}$ for 66VP82P samples. Thermoelectric power studies revealed that the charge carriers are the Ag⁺ ions, with an activation energy of 0.288 eV for 66VP82G, which correlated well with the activation energy obtained from the conductivity measurements. The dielectric constant, dielectric loss and the loss tangent were calculated for both polycrystalline and glassy 66VP82 material. It was observed that the dielectric loss is more for the glassy material than the polycrystalline material. Solid state galvanic cells with 66.6% AgI-22.2% Ag₂O-11.1% V₂O₅, 66.6% AgI-22.2% Ag₂O-11.1% P₂O₅ and 66.6% AgI-22.2% Ag₂O-11.1% (0.8 V₂O₅-0.2 P₂O₅) (coded as 66V, 66P and 66VP82 respectively) electrolytes were constructed. Both polycrystalline and amorphous electrolyte cells were fabricated for a comparative study and the polarization effects were observed to be negligible in amorphous cells. The variation of open circuit voltage with temperature was reported and the current discharge curves indicate that the 66VP82 material has higher current capacity with high current drain when compared to 66V and 66P cells.

1. Introduction

The unique transport properties of solid electrolytes (high ionic conductivity and relatively small electronic conductivity) and their application to solid state batteries, electrochemical analogue memory devices, electrochemical capacitors, solid electrolyte coulometers and sensors have attracted a great deal of attention to the study on the electrical and dielectric properties of silver iodide-silver oxide based polycrystalline and glassy materials with a host of glass formers of the type M₂O₅ (M = vanadium, phosphorous, arsenic). The Zachariasen criterion [1] for glass formation is where a three-dimensional network, lacking long range periodicity, with no oxygen atom linked to more than two metal atoms and, with a minimum number of oxygen atoms around the metal atom and the oxygen polyhedra sharing corners with each other, than the edges or the faces that form the three-dimensional glass network. The following system of quarternary

compounds AgI-Ag₂O-V₂O₅-P₂O₅, AgI-Ag₂O-P₂O₅-As₂O₅ and AgI-Ag₂O-As₂O₅-V₂O₅ are chosen for a detailed study of transport and dielectric properties in all possible compositions. Although Minami *et al.* [2] established the glass formation region in the ternary systems AgI-Ag₂O-P₂O₅ and AgI-Ag₂O-V₂O₅ with an assumption that two glass formers will form a better glass with high random glass matrix, the effect of a glass modifier on the ionic conductivity in a quarternary system has been reported [3]. It was found that for a glass former (GF) to glass modifier (GM) ratio of 0.5, the best conducting composition obtained was 66.6% AgI-22.2% Ag₂O-11.1% (V₂O₅-P₂O₅). Then fixing the GF to GM ratio as 1:2, the internal composition of V₂O₅ and P₂O₅ was varied and the transport and dielectric studies were reported. It was found that 66.6% AgI-22.2% Ag₂O-11.1% (0.8 V₂O₅-0.2 P₂O₅) has the highest conductivity. A detailed analysis of the a.c. and d.c. conductivities in

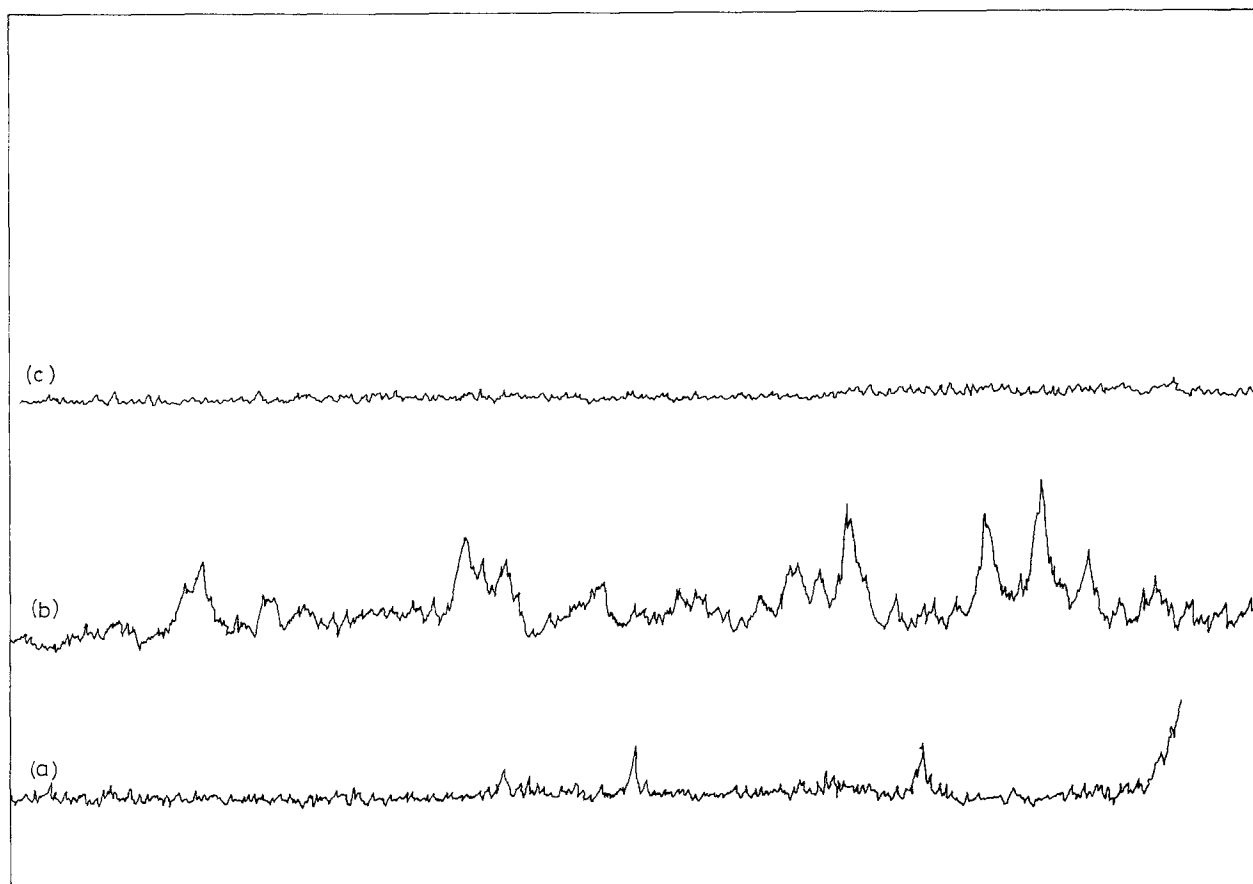


Figure 1 X-ray diffractogram of the (a) amorphous nature of the substance formed in the quartz tube after rapid quenching of the vacuum sealed quartz tube. (b) amorphous nature of the substrate formed in the quartz tube by the starting materials method. (c) Amorphous nature of the substance formed by the open air crucible method.

AgI-Ag₂O-V₂O₅-P₂O₅ glasses will be presented elsewhere [4], while the preliminary investigation using the best conducting composition 66.6% AgI-22.2% Ag₂O-11.1% (0.8 V₂O₅-0.2 P₂O₅) as an electrolyte material for a solid state battery is reported here.

2. Preparation

In a previous communication [3], where electrical and dielectric studies on superionic conducting AgI-Ag₂O-V₂O₅-P₂O₅ quaternary systems were attempted, the methods of preparation of both polycrystalline and glasses from the same melt were explained there briefly. It was found that the technique of open air crucible melting (for polycrystalline) followed by rapid quenching (for glassy) has the advantages of uniform, stoichiometric contents of the starting materials, low activation energy and enhanced conductivity. Here, a detailed explanation of the three methods of preparation is given in order to highlight the effect of sample preparation on the electrical properties and particularly on the electrochemical cell performance.

2.1. Vacuum sealed quartz tube quenching method

In this method of preparation, analar grade AgI, Ag₂O, V₂O₅ and P₂O₅ (Fluka, analar grade) were weighed to the desired composition in an electropan balance and transferred into a dry box. The mixture was well mixed by grinding, transferred into a quartz tube and heated away from the charge. A small capil-

lary opening was drawn through which small residual traces of moisture could escape. It was observed that there was a slight loss of P₂O₅ and I₂ because of exothermicity in the reaction. Hence a small quantity of H₂O was deliberately added to the weighed amount in order to control the rate of process. Then the quartz tube was vacuum sealed and the mixture melted and homogenized in an electrical muffle furnace kept at a constant temperature of 500° C with a temperature controller to an accuracy of ± 5° C. The clear reddish yellow orange melt in the quartz tube was subsequently quenched in a column containing liquid nitrogen. The X-ray diffractogram of the glassy material obtained is shown in Fig. 1 which confirms the amorphous nature of the sample. However, as the diffractogram contains small peaks, it can be concluded that slight traces of a polycrystalline nature exists. This can be attributed to the quenching method which is not instantaneous. By the time the compound attains the required quenching rate for the formation of glass in the quartz tube, crystallization takes place in the core of the material. In this method only the pulverized glass was used to study the ionic conductivity and bulk glass studies were not attempted as it was very difficult to cut the glass mould into a regular shape, as the glass is very fragile.

2.2. Melt from the starting materials

In this method of preparation, the calculated quantities of AgNO₃, KI, Ag₂O, NH₄H₂PO₄ and V₂O₅ were mixed and melted at 200° C to form AgI-Ag₂V₂O₆-

$\text{Ag}_2\text{P}_2\text{O}_6$. This was followed by heating the melt at 500°C for 3 h in an electrical muffle furnace with a temperature controller to an accuracy of $\pm 5^\circ\text{C}$. Regular stirring of the melt in the crucible ensured a homogeneous mixture. The melt was quenched onto a silver plate which kept at liquid nitrogen temperature. A small amount of the compound was removed at 200°C and an X-ray diffractogram was taken to check the formation of polycrystalline $\text{AgI-Ag}_2\text{V}_2\text{O}_6\text{-Ag}_2\text{P}_2\text{O}_6$. It was found that no such compound existed and this confirms the formation of a quarternary rather than a ternary system.

2.3. Open air crucible quenching method

This preparation involved quite a different method, as was adopted by Minami *et al.* [2]. The glassy material $\text{AgI-Ag}_2\text{O-P}_2\text{O}_5$ was prepared in a vacuum sealed annealing tube at a temperature of 350°C for 6 h and then directly quenched in liquid nitrogen. The calculated amounts of the compounds AgI , Ag_2O , V_2O_5 and P_2O_5 for the required composition were weighed and then mixed well by grinding in a mortar with a pestle. The crucible containing this mixture was kept in a vertical open end electrical muffle furnace for 3 h at a temperature of 450°C in open air. The crucible was stirred occasionally to ensure a homogeneous melt formation. The melt was then rapidly quenched in a column of liquid nitrogen. The glass was allowed to reach room temperature by exposing it to open air for 12 h and it was then pulverized. The pulverized glass powder was made into pellets of 1.3 cm diameter and 0.3 cm thickness. In this method, bulk glasses were obtained by pouring the melt in stainless steel moulds kept at liquid nitrogen temperature.

The samples were annealed below the glass transition temperature for a protracted period of time, in order to allow mechanical stress relaxation and configurational relaxation to take place. There is a reduction in volume, since the glass relaxes to a more stable state after which the charge carriers will be homogenized.

3. Ionic conductivity

Both the $\text{AgI-Ag}_2\text{O-P}_2\text{O}_5$ and $\text{AgI-Ag}_2\text{O-V}_2\text{O}_5$ glassy and polycrystalline compounds have been well studied [5, 6]. In these ternary systems, the glass former to glass modifier ratio was changed and the best conducting compositions were established as mol % 66.6 $\text{AgI-22.2 Ag}_2\text{O-11.1 P}_2\text{O}_5$ and 66.6 $\text{AgI-22.2 Ag}_2\text{O-11.1 V}_2\text{O}_5$. The compositional dependence of the conductivity σ , on AgI mol %, for the systems $\text{AgI-Ag}_2\text{O-P}_2\text{O}_5$ and $\text{AgI-Ag}_2\text{O-V}_2\text{O}_5$ was well established. The conductivity $\log \sigma T$ increases as the AgI content increases up to 66%, and decreases thereafter indicating that only 66% of AgI actively involves itself in the transport process. Hence in the present system, 66.6% $\text{AgI-22.2% Ag}_2\text{O-11.1% ((1-x) V}_2\text{O}_5\text{-x P}_2\text{O}_5)$ was used to study the temperature dependence of the conductivity. Since two glass formers are involved, the variation of glass former composition with $(1-x)$ $\text{V}_2\text{O}_5\text{-x P}_2\text{O}_5$ for $0.1 < x < 0.9$ was studied and the best conducting composition was established to be 66.6% $\text{AgI-22.2% Ag}_2\text{O-11.1% (0.8 V}_2\text{O}_5\text{-0.2 P}_2\text{O}_5)$

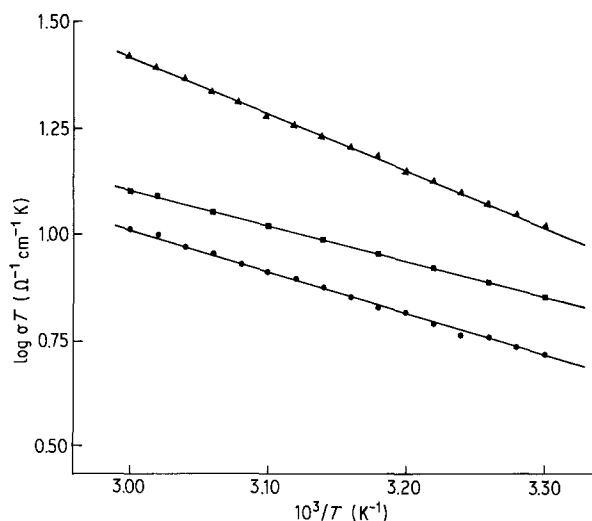


Figure 2 $\log \sigma T$ against $10^3/T$ plots for the mol % (■) 66.6 $\text{AgI-22.2 Ag}_2\text{O-11.1 V}_2\text{O}_5$, (●) 66.6 $\text{AgI-22.2 Ag}_2\text{O-11.1 P}_2\text{O}_5$ and (▲) 66.6 $\text{AgI-22.2 Ag}_2\text{O-11.1 (0.8 V}_2\text{O}_5\text{-0.2 P}_2\text{O}_5)$ glasses.

and has been reported elsewhere [7]. In Fig. 2 a comparison of conductivity between mol % 66.6 $\text{AgI-22.2 Ag}_2\text{O-11.1 P}_2\text{O}_5$ and 66.6 $\text{AgI-22.2 Ag}_2\text{O-11.1 V}_2\text{O}_5$ is shown. For the composition mol % 66.6 $\text{AgI-22.2 Ag}_2\text{O-11.1 (0.8 V}_2\text{O}_5\text{-0.2 P}_2\text{O}_5)$ an enhancement of conductivity was observed with relatively low activation energy. This proves our assumption that a combination of glass formers forms a better fast ion conducting glass. This result has motivated us to make a complete study of the quarternary superionic conducting systems whose ionic conductivity can also be expressed by the relation

$$\sigma = \sigma_0/T \exp(-E/kT)$$

where σ_0 is a constant, T the absolute temperature, k Boltzmann's constant and E the activation energy for Ag^+ ion conduction. The activation energy of the sample was calculated from the slope of the plot $\log \sigma T$ against $10^3/T$.

The comparison of ionic conductivity between bulk glasses and pellets for the same composition is shown in Fig. 3. It was observed in the present study that

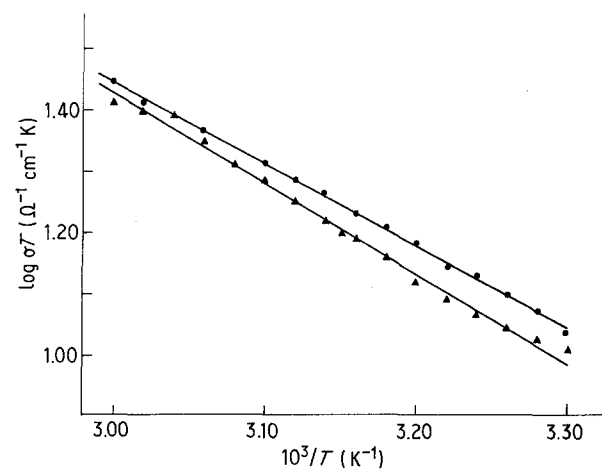


Figure 3 Plots of $\log \sigma T$ against $10^3/T$ for the superionic conducting electrolyte mol % 66.6 $\text{AgI-22.2 Ag}_2\text{O-11.1 (0.8 V}_2\text{O}_5\text{-0.2 P}_2\text{O}_5)$ in the form of bulk glass (● 66VP82B thickness 0.324 cm, $E_a = 0.242\text{ eV}$) and pulverized glass (▲ 66VP82 thickness 0.375 cm, $E_a = 0.298\text{ eV}$).

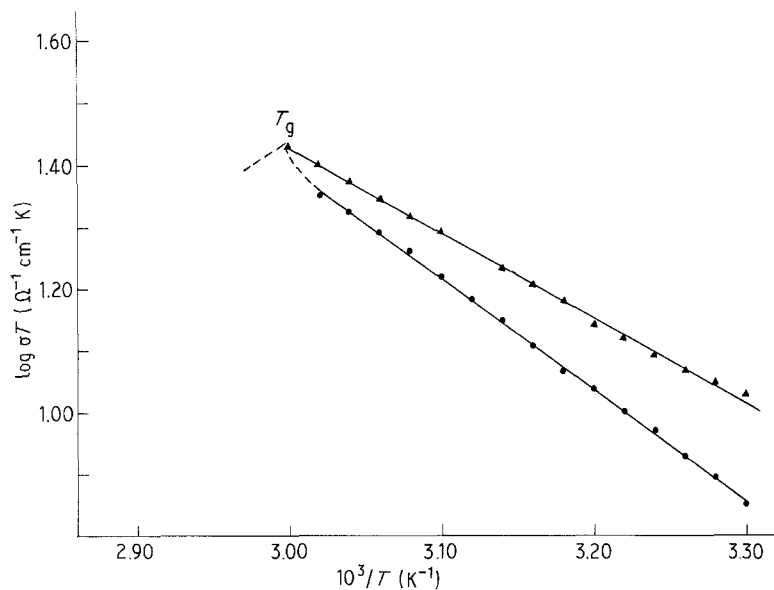


Figure 4 Illustration of the temperature dependence of $\log \sigma T$ on $10^3/T$ (▲) for the glass 66VP82 ($E_a = 0.298$ eV) on heating cycle and (●) for the polycrystalline 66VP82 ($E_a = 0.346$ eV) on the cooling cycle.

the conductivities of pellets at a given temperature are lower than those of bulk glasses whereas the activation energies are almost the same. Fig. 4 shows the comparison of temperature dependence of conductivity between the glassy and polycrystalline samples, where polycrystalline nature was observed after the glassy sample temperature was raised above the glass transition temperature (T_g). This was also confirmed from the X-ray diffractogram taken after annealing the sample above the glass transition temperature for 3 h as shown in Fig. 5. It was observed that the activation energy of the polycrystalline

material was higher than that of the glassy material agreeing well with the observed results of AgI-Ag₂O-P₂O₅ and AgI-Ag₂O-V₂O₅ ternary systems. The furnace was switched off once the glass transition temperature was reached and the readings for the polycrystalline sample were taken on the cooling cycle. Thus the glass is not annealed above the glass transition temperature. Even then the glassy material becomes polycrystalline as can be seen from the diffractogram shown in Fig. 5. Fig. 5, (1) shows the diffractogram of the amorphous sample, (2) shows the diffractogram at the glass transition temperature and

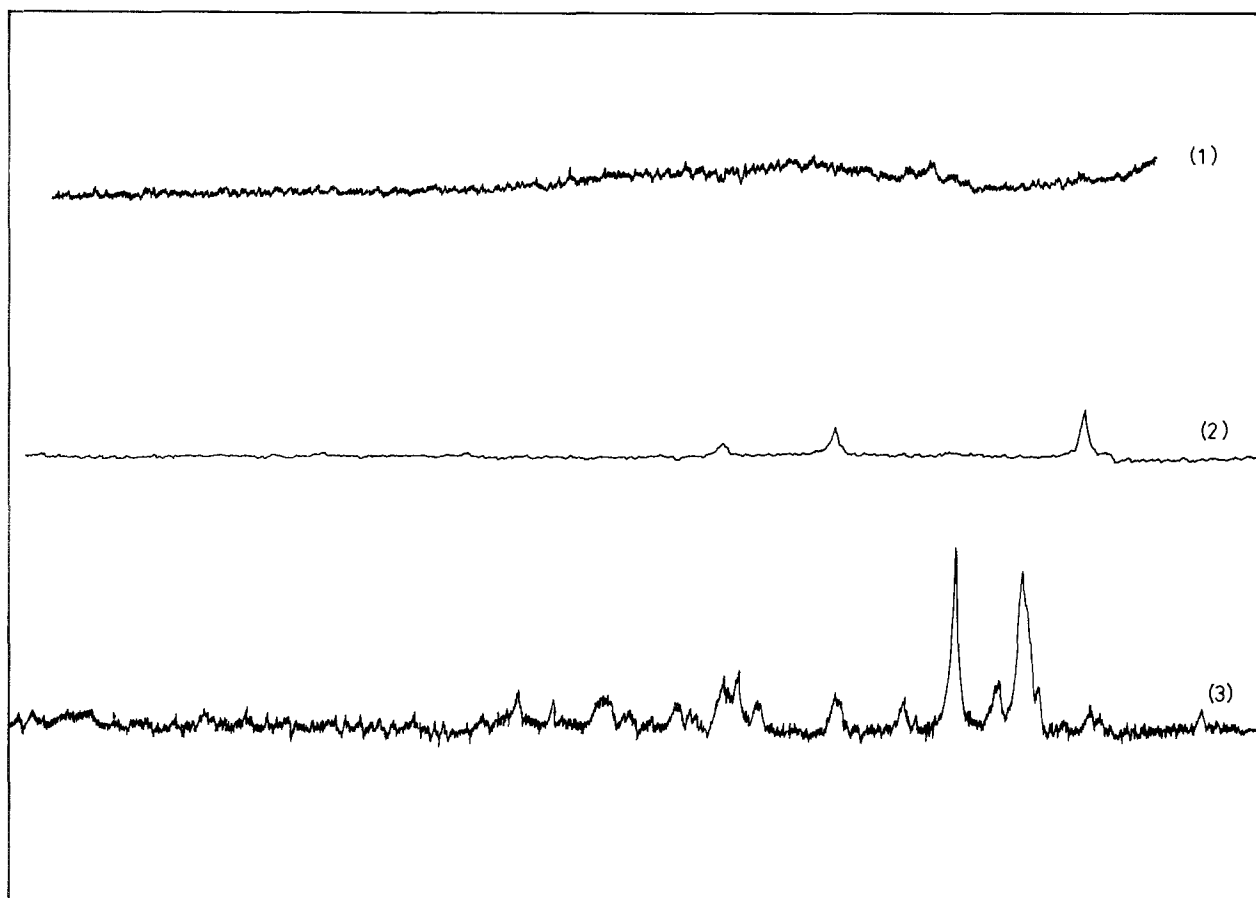


Figure 5 X-ray diffractogram of the glass (1) before the heating cycle and (2) after reaching the glass transition temperature and (3) after the cooling cycle.

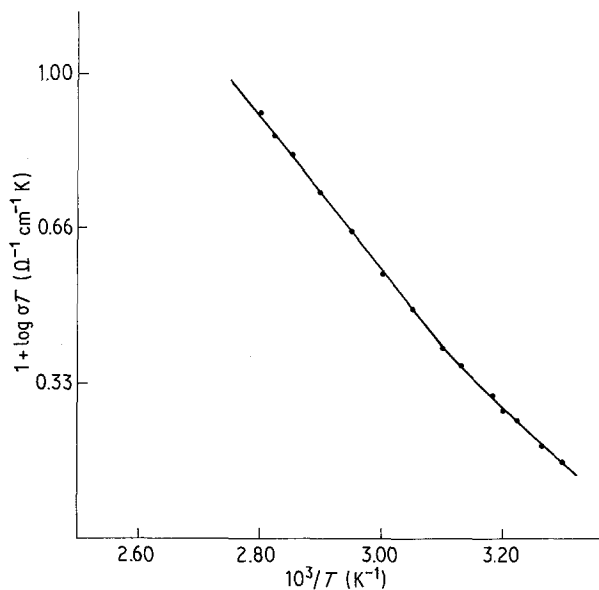


Figure 6 Illustration of the temperature dependence of $\log \sigma T$ for the polycrystalline sample 66VP82P ($E_a = 1.471$ eV).

(3) is the diffractogram after the completion of the heating and cooling cycle. In Fig. 6, the temperature dependence of conductivity for the polycrystalline sample is shown, from which it is evident that the sample undergoes a phase transition from the glassy state to a polycrystalline state. The activation energy increases for the polycrystalline sample with a decrease in the conductivity. Thus the amorphous sample behaves as a polycrystalline material above the glass transition temperature.

The variation of resistance with time for the polycrystalline (1) bulk glass (2) and pulverized glass (3) was plotted in Fig. 7. The variation of resistance with time is large for the pulverized glass pellet when compared to the bulk glass. This conforms with the established fact that the stress induced on the application of pressure to make the pellet, relaxes after some time and hence the resistance increases. The resistance of the polycrystalline sample stabilized within 2 h, whereas the glassy samples stabilized in 12 h. This once again confirms that more time is required for the pelletized glass than the polycrystalline as the glass undergoes more mechanical strain due

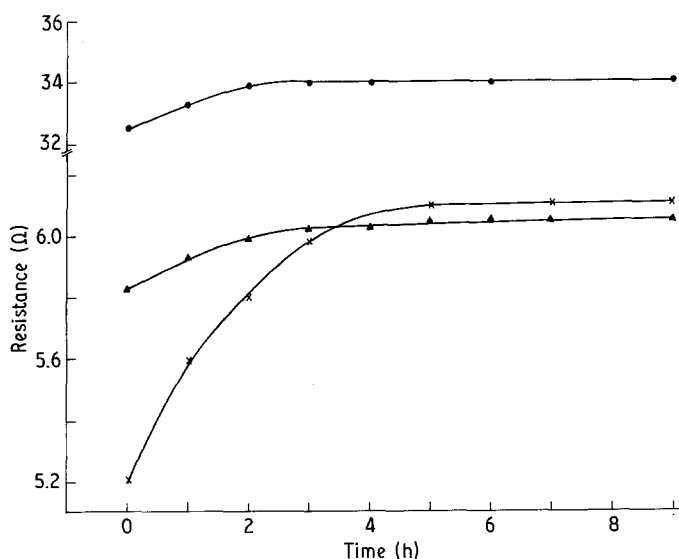


Figure 7 Plot of variation of resistance (Ω) against time (h) for (●) the polycrystalline, (▲) the bulk glass and (×) pulverized samples until the resistance stabilises to a constant value.

to the pellet pressing. The variation of resistance with frequency for the pulverized glass is shown in Fig. 8. The resistance increases generally from 1.0 to 100 Hz and then drastically decreases up to 1.0 kHz and then is quite stable in the region 1.0–100 kHz. A further drop in resistance is observed from 100 kHz to 1.0 MHz. The nature of this resistance dependence on frequency is generally attributed to the electrode–electrolyte interface capacitance effects. However we intend to study it in detail by studying the IR and Raman spectra, from which the formation of ionic clusters can be confirmed rather than the condensed structural units in the glass [8].

Hence from the above ionic conductivity measurements, the conductivity for the sample 66.6% AgI–22.2% Ag_2O –11.1% ($0.8 \text{ V}_2\text{O}_5$ – $0.2 \text{ P}_2\text{O}_5$) coded as 66VP82, in the bulk form was obtained as $4.18 \times 10^{-2} \Omega^{-1} \text{ cm}^{-1}$ at 300 K and in the pulverized form as $3.16 \times 10^{-2} \Omega^{-1} \text{ cm}^{-1}$ at 300 K. The polycrystalline sample conductivity was obtained as $8.13 \times 10^{-3} \Omega^{-1} \text{ cm}^{-1}$ at 300 K. The glass transition temperature in both the amorphous samples (bulk and pulverized) was observed to be 60°C .

4. Electronic conductivity

Wagner's polarization cell of the configuration (–) Ag/Electrolyte/C(+) was used to determine the electronic contribution to the total conductivity. Here silver is used as an anode and graphite powder as a cathode. When the d.c. potential (from 10 to 200 mV) was applied to the above configuration, the flow of silver ions due to the electrical potential difference will equal the flow due to the chemical potential and the total current will be transported by electrons or holes only, as the ionic motion is blocked by the blocking electrode graphite. If V is the applied potential, then the total current is given by

$$I = I_e + I_h$$

$$I = \frac{RTA}{LF} \sigma_e \left[1 - \exp\left(\frac{-VF}{RT}\right) \right] + \sigma_h \left[\exp\left(\frac{VF}{RT}\right) - 1 \right]$$

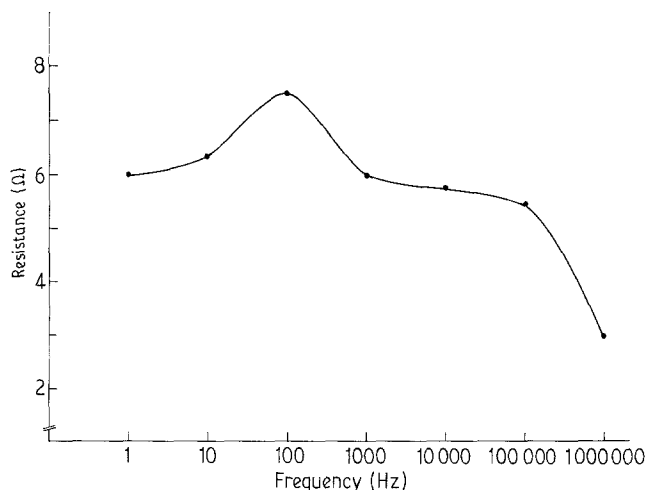


Figure 8 Plot of the variation of resistance (Ω) against frequency (Hz) in decade steps for 66VP82 glass sample (thickness 0.375 cm).

where I_e and I_h are the components of electric current due to electrons and holes respectively, R is the gas constant, T the temperature, A the area of cross section, L the thickness of the pellet, F the Faraday constant and V the applied potential.

When the applied voltage V is sufficiently high satisfying the condition $VF \gg RT$; then we have

$$I = I_e = \frac{RTA}{LF} \sigma_e$$

and

$$I = I_h = \frac{RTA}{LF} \exp\left(\frac{VF}{RT}\right) \sigma_h$$

Fig. 9 shows the I - V plot for the 66VP82 glassy (1) and polycrystalline (2) samples. When $[1 - \exp(-VF/RT)]$ against I is plotted, the slope directly gives the value RTA/LF . Hence the electronic conductivity can be calculated directly. It is observed from the I - V curves, that the current increases with an increase in the applied voltage until 120 mV, as shown in Fig. 9 which explains the equations mentioned above. It is seen that the current remains constant above 140 mV. The variation of current (I) is linear in two regions of voltages, 20–80 mV and 100–140 mV. Thus the calculated electronic conductivity for the bulk sample, pellet and polycrystalline 66VP82 are 2.25×10^{-10} , 6.24×10^{-10} and $3.8 \times 10^{-8} \Omega^{-1} \text{cm}^{-1}$ respectively.

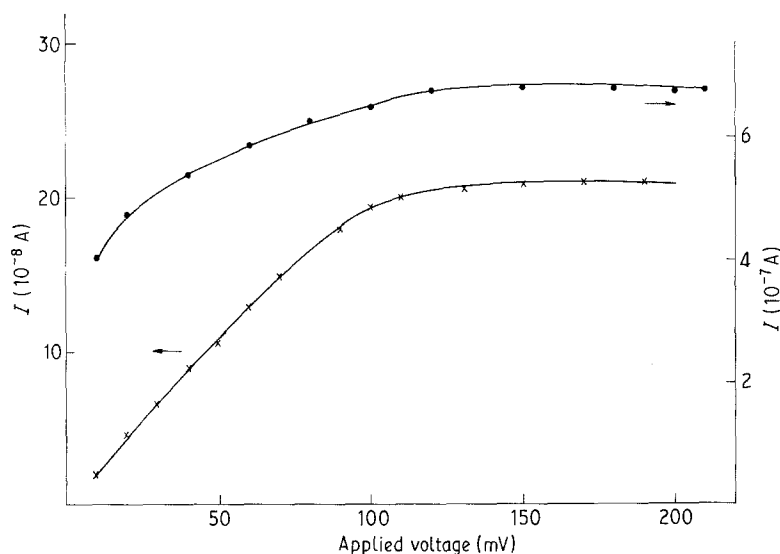


Figure 9 Illustration of the I - V characteristics curves for the 66VP82 (x) amorphous and (●) polycrystalline samples ($E_a = 0.288 \text{ eV}$).

5. Thermoelectric power

In the AgI-based solid electrolytes, Ag^+ ions are the mobile species and the contribution of electronic conductivity to the total conductivity is found to be negligible. Hence the predominant conducting species are Ag^+ ions and hence ionic conductivity takes place. When a temperature gradient is maintained across the pellet, a voltage appears across the pellet due to the flow of silver ions within the pellet. The ratio of the thermoelectric voltage (ΔV) developed due to the temperature gradient (ΔT) is known as the thermoelectric power (S). Thus

$$-S = \Delta V / \Delta T$$

The sign convention used in the present investigation is that S is positive if the hot end is positive and vice versa. When the thermodynamical steady state is reached, the sign of the voltage across the pellet represents the sign of the electric charge on the mobile species. Hence thermodynamic power is an important tool for determining the nature of the charge carriers. These studies will also provide information about the number and type of defects, their mobility and the heat of transport. With a view to confirming the mobile carriers in the glassy electrolyte $\text{AgI-Ag}_2\text{O-V}_2\text{O}_5\text{-P}_2\text{O}_5$ and the sign of the mobile charges, the measurements of thermoelectric power and electrical conductivity have been carried out in the present investigation.

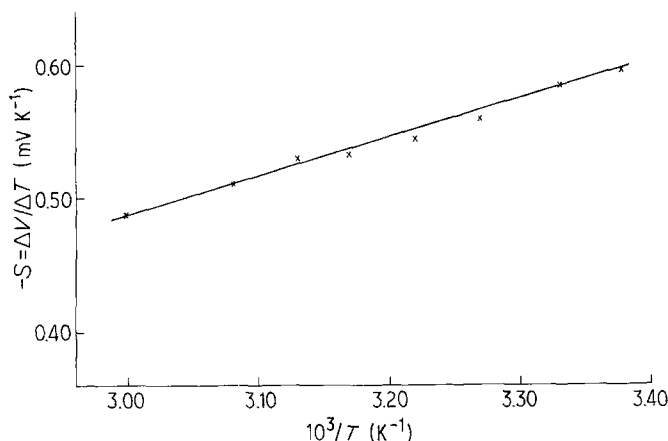


Figure 10 Dependence of the calculated thermoelectric power, S , on the variation of temperature for 66VP82 glass sample.

The measurements of thermoelectric power at various temperatures were carried out on the above pellet. A constant temperature gradient of 10 K was maintained across the pellet and the dependence of S on temperature is shown in Fig. 10. It can be seen from the above figure that the magnitude of the thermoelectric power decreases as the temperature increases which was also observed by earlier workers [9–11] for superionic conductors. The value of thermoelectric power obtained in the present investigation is negative and hence the mobile carriers are positively charged Ag^+ ions. Since silver electrodes are used in the present investigation, the inhomogeneous contribution of thermoelectric power to the total thermoelectric power is eradicated [11]. Thus the activation energy due to the heat of transport as obtained from the plot of $-S$ against $10^3/T$ is 0.288 eV, which coincides well with the activation energy of migration as obtained from the ionic conductivity $\log \sigma T$ against $10^3/T$ plot. Thus it can be concluded that the charge carriers are Ag^+ ions with an activation energy of 0.288 eV.

6. Dielectric constant, dielectric loss and loss tangent

By measuring the capacitance of the pellets, the relative dielectric constant K' for the samples in the form of pellets was calculated using the equation

$$K' = \frac{\text{Thickness}}{0.0885 \times \text{Area}} \times \text{capacitance}$$

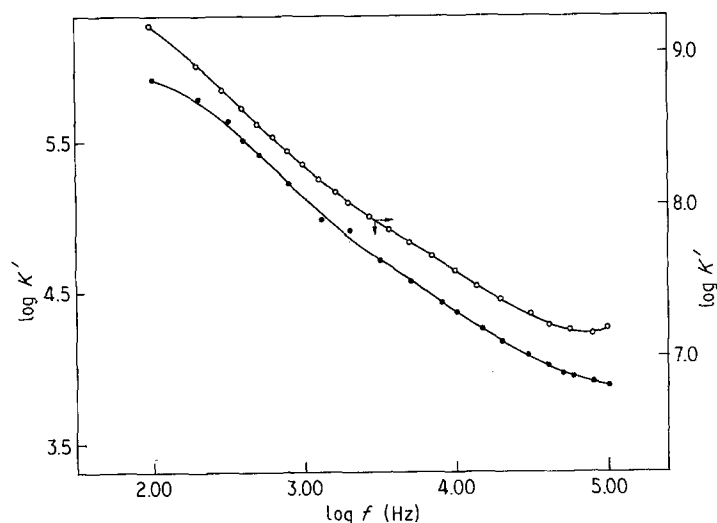


Figure 11 Illustration of the dependence of the dielectric constant K' on frequency for (○) polycrystalline 66VP82 and (●) amorphous 66VP82 samples.

where the thickness is in cm, the area in cm^2 and the capacitance in PF. The relative dielectric loss K'' was calculated from the equation

$$K'' = K' \tan \delta$$

The loss tangent, $\tan \delta$ was directly measured from the bridge and used to calculate the dielectric loss.

The variation of dielectric constant ($\log K'$) with frequency for the polycrystalline and glassy 66VP82 sample is shown in Fig. 11(a) and 11(b) respectively. At 100 Hz, the dielectric constant K' and dielectric loss for the polycrystalline 66VP82 were 1.56×10^9 and 1.74×10^{10} respectively as compared with 1.26×10^6 and 1.803×10^7 respectively for the glassy 66VP82. For the polycrystalline and glassy 66VP82, there is an order of magnitude difference of 3. In both forms, the dielectric loss is approximately ten times more than the dielectric constant. In the case of polycrystalline 66VP82, it can be observed from Fig. 11(a), that the variation of K' in the higher (10–100 kHz) and lower (10–500 Hz) frequency ranges is exponential and linear in the 500–8000 Hz frequency range. No such behaviour was observed in the glassy 66VP82. The behaviour of polycrystalline 66VP82 is very similar to that of AgI [12] and in the glassy 66VP82 a slight anomaly was observed. This can be attributed to the randomness in the glassy matrix, whereas in the polycrystalline case, the value of K' decreases with increasing frequency. This shows that AgI content is more responsible for the dielectric constant or loss

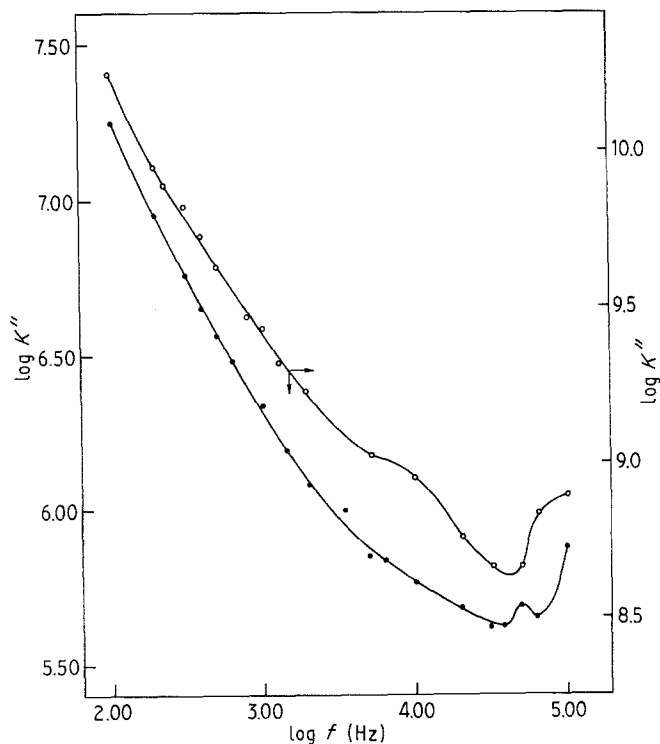


Figure 12 Illustration of the dependence of dielectric loss K'' on frequency for (○) polycrystalline 66VP82 and (●) amorphous 66VP82 samples.

indicating that the dielectric constant of the material is still related to the electronic, ionic dipolar and space charge polarizations. Whereas for the glassy 66VP82, the contribution seems to be only from ionic conductivity. The dielectric loss for polycrystalline and glassy 66VP82 sample is shown in Fig. 12(a) and 12(b) respectively.

The values of the dielectric loss for polycrystalline and glassy 66VP82 at 100 Hz and 100 kHz are 1.74×10^{10} , 7.26×10^8 , 1.80×10^7 and 7.77×10^5 , respectively.

In both the polycrystalline and glassy forms the dielectric loss decreases rapidly as the frequency increases indicating that the dielectric loss contribution is due to the high ionic conductivity of the samples. The contribution of dielectric loss due to the space charge polarization is negligible in the glassy form and comparatively high in the polycrystalline form since the space charge contribution depends on

the purity and perfection of the crystallinity. Hence this conforms with the observation of a lower dielectric loss for glassy 66VP82 than for the polycrystalline 66VP82, where perfection is more in polycrystalline samples than glass.

The dependence of $\log \tan \delta$ on frequency for the polycrystalline and glassy 66VP82 samples is shown in Fig. 13(a) and 13(b) respectively. As can be observed from Fig. 13(a) for the polycrystalline sample, the variation is exponential and uniform. In the case of glassy material as can be seen from Fig. 13(b) the variation is not exponential but slightly linear in the 100 Hz–10 kHz region and then exponential from 10–100 kHz. When $\log \tan \delta$ is plotted against \log frequency, an exponential curve is obtained. This is an indication that the charged defects due to the space charge polarization in the polycrystalline material contribute to the total dielectric loss whereas in glassy material, the space polarization contribution is less.

Hence from the above dielectric studies it can be concluded that although the difference in order of magnitude of ionic conductivity in the case of polycrystalline and amorphous material is not much, there is a three orders of magnitude difference in the dielectric constant and dielectric loss. This is an indication of the extent of the space charge polarization and electronic conductivity contribution to the dielectric constant and loss factor. From the preliminary investigation it can be concluded that in the case of the polycrystalline sample, the high dielectric constant and dielectric loss in the polycrystalline 66VP82 are due to the contribution from the low electronic conductivity, dipolar and space charge polarization. The comparatively low dielectric constant and dielectric loss for the glassy material can be explained by the low electronic and high ionic conductivity with almost negligible contribution from the space charge polarization. Hence a definite conclusion can be

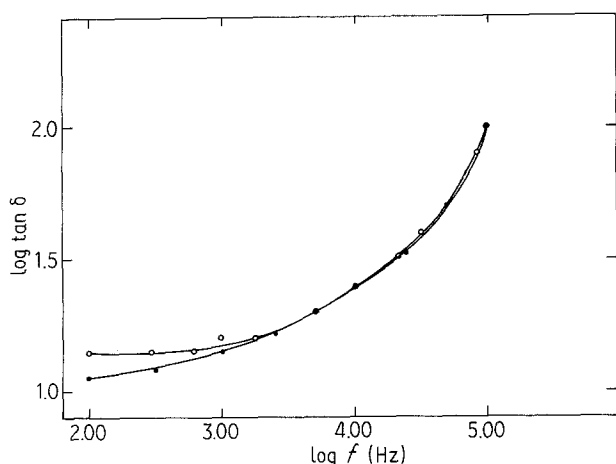


Figure 13 Illustration of the dependence of loss tangent, $\tan \delta$ on frequency for (●) polycrystalline 66VP82 and (○) amorphous 66VP82 samples.

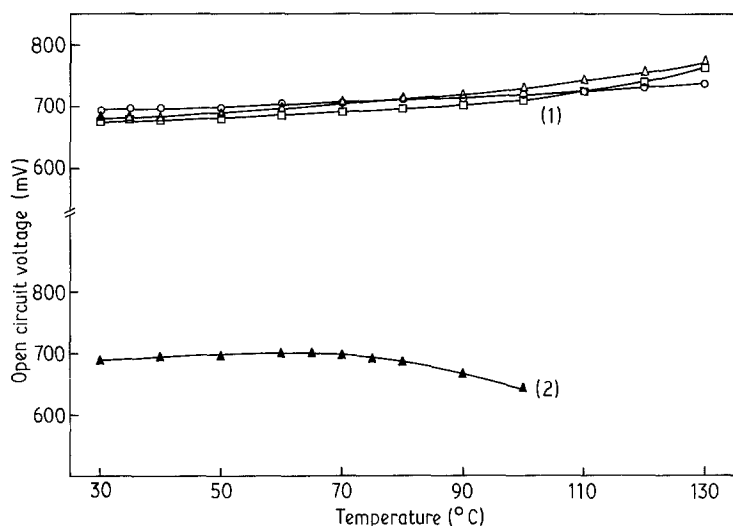


Figure 14 Illustration of the variation of open circuit voltage with increasing temperature: Curves (1) are for polycrystalline electrolyte cells with (○) AgI–Ag₂O–V₂O₅ (□) AgI–Ag₂O–P₂O₅ and (Δ) AgI–Ag₂O–V₂O₅–P₂O₅, Curve (2) is for amorphous electrolyte cell with (▲) AgI–Ag₂O–V₂O₅–P₂O₅.

given only when the dielectric properties are studied in the 0.1–100 Hz and 100 Hz–10 MHz ranges also with a temperature variation of the dielectric loss K'' at a particular frequency. The small variation of dielectric constant and loss with an increase in frequency at low frequencies indicates that the silver ion migration on the surface of glass is negligible. Moreover a thorough investigation of the dielectric property of the combination of V₂O₅ and P₂O₅ in the glassy matrix, will give a better understanding of the effect of V₂O₅–P₂O₅ on the ionic conduction mechanism and the assumption that the difference in the polarizabilities of V⁵⁺ and P⁵⁺ is the factor that influences and enhances the ion migration thus enhancing the ionic conductivity.

7. Solid state cells

A great deal of success has been met with the invention of glassy electrolytes and some of the above disadvantages are overcome to a certain extent. At the same time, efforts are being made to find new cathode materials which can increase the shelf-life of the battery with a high stability in the open circuit voltage and a constant current. Hence an attempt is made to fabricate cells using the best conducting composition mol % 66.6 AgI–22.2 Ag₂O–11.1 (0.8 V₂O₅–0.2 P₂O₅) glassy electrolyte with I₂ (iodine + graphite) powder as a cathode and compare its current discharge and load characteristics performance with that of mol % 66.6 AgI–22.2 Ag₂O–11.1 V₂O₅ and mol % 66.6 AgI–22.2 Ag₂O–11.1 P₂O₅ cells.

7.1. Fabrication

Four cells of each electrolyte with polycrystalline and amorphous material of composition mol % 66.6 AgI–22.2 Ag₂O–11.1 V₂O₅, 66.6 AgI–22.2 Ag₂O–11.1 P₂O₅ and 66.6 AgI–22.2 Ag₂O–11.1 (0.8 V₂O₅–0.2 P₂O₅) were fabricated in the form of cylindrical pellets under a pressure of 6000 kg cm⁻² with a diameter of 1.0 cm and a thickness of 0.5 cm. The contact polarization effects at the anode–electrolyte interface were reduced by incorporating a mixture of electrolyte and 200 mesh silver powder in the anode structure. The best performance of the open cell voltage and current discharge characteristic curve was obtained for the

cells with the weight ratios of anode, electrolyte and cathode as shown below.

Anode: 0.4 g of electrolyte with 0.15 g of silver powder.

Electrolyte: 1.0 g of electrolyte.

Cathode: 0.4 g of electrolyte with 0.4 g of iodine and 0.07 g of graphite powder.

Hence the cell configuration is

(Ag + Electrolyte)/Electrolyte/

(I₂ + Carbon + Electrolyte)

After the fabrication of the cells, an independent study of the performance of the open circuit voltage with temperature, the current discharge characteristic curves and load characteristic curves for the optimum discharge current of 0.5 mA was undertaken. An attempt was made to prove the advantages of amorphous electrolytes over the polycrystalline and only the load characteristic curves of amorphous electrolyte cells were shown here.

7.2. Open circuit voltage

The open circuit voltage (OCV) of all the polycrystalline electrolyte cells are shown in Fig. 14 (1). The measured OCV of the cell was compared to that of the pure AgI and the transport number was determined. The polycrystalline electrolyte cell with AgI–Ag₂O–V₂O₅ electrolyte has the highest OCV of 0.686 V and the cell with AgI–Ag₂O–P₂O₅ electrolyte 0.682 V. The polycrystalline electrolyte cell with AgI–Ag₂O–V₂O₅–P₂O₅ electrolyte has an OCV of 0.684 V as can be seen in Fig. 14 (1). The temperature variation of OCV was shown for the three polycrystalline cells in Fig. 14. In the case of amorphous electrolyte cell, as shown in Fig. 14 the OCV of the cell with AgI–Ag₂O–V₂O₅–P₂O₅ electrolyte decreases slowly after the glass transition temperature. This is the first time such an observation has been reported. This can be attributed to the formation of polycrystalline material and hence a reduction in the ionic conductivity of the mobile cation. Thus the transport number decreases, and hence the decrease in the OCV. It can be concluded that this particular amorphous electrolyte is unstable above the glass transition temperature of 70 °C.

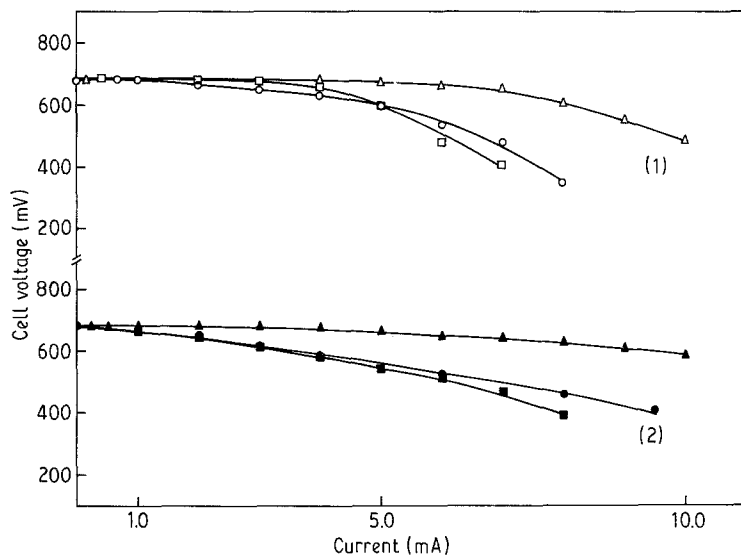


Figure 15 Illustration of the current discharge characteristic curves (1) for polycrystalline electrolyte cells and (2) for amorphous electrolyte cells. Here \circ and \bullet correspond to polycrystalline and amorphous $\text{AgI-Ag}_2\text{O-V}_2\text{O}_5$ systems respectively. \square and \blacksquare correspond to polycrystalline and amorphous $\text{AgI-Ag}_2\text{O-P}_2\text{O}_5$ systems respectively and \triangle and \blacktriangle correspond to polycrystalline and amorphous $\text{AgI-Ag}_2\text{O-V}_2\text{O}_5\text{-P}_2\text{O}_5$ systems respectively.

7.3. Current discharge characteristics

The specific energy is the parameter used for assessing the relative cell performance with $(\text{Ag} + \text{electrolyte})/\text{Electrolyte}/(\text{I}_2 + \text{carbon} + \text{electrolyte})$ configuration. Thus the polycrystalline and glassy electrolytes were pressed with anode and cathode to form the cells and their current discharge curves at 30°C are shown in Fig. 15 (1) and (2) respectively. The capability of sustaining a large current drain without undue polarization is specified by the power rating of the cell. As can be seen in Fig. 15 (1) and (2), the cell with 66VP82 (\triangle) has a higher power rating than those for 66V (\circ) and 66P (\square) cells. When current is drawn from the cell, the power initially rises, it reaches a maximum and then drops. This is more clearly seen in the case of cells with polycrystalline electrolytes, as shown in Fig. 15 (1). This can be attributed to the polarization effects. Hence in amorphous electrolyte cells, the polarization effects are negligible and this is one of the advantages of using amorphous electrolytes in solid state batteries.

In the present investigation, very little attention has been paid to any particular application. Hence, a general purpose application is assumed, where the cell need not have to undergo instantaneous power discharge. Also short discharges are avoided as the maximum premitted continuous power level is found

to be appreciably high in the case of 66VP82 electrolyte cells. This might be one of the reasons why mass and transport polarization effects are less significant for short discharges and the quarternary cells are not prone to thermal instability and permanent damage. Hence from the polarization performance curves shown in Fig. 15 (1) and (2), detailed information on the characteristic behaviour of cells under load and at various stages of discharge could not be obtained. Thus the cell voltage as a function of the fraction of discharge completed, known as discharge curves are plotted with discharge rate at 0.5 mA for all cells.

7.4. Load discharge characteristics

Fig. 16 shows the load discharge curves for the three amorphous electrolyte cells 66V (\bullet), 66P (\blacksquare) and 66VP82 (\blacktriangle) with a constant load resistor $1.2\text{ k}\Omega$ rated at 0.25 W . It is observed that at a current drain of 0.5 mA , the continuous discharge time is approximately 16h for the amorphous 66VP82 electrolyte cell and comparatively less for both the amorphous 66V and 66P electrolyte cells. Hence the calculated cell capacity is about 16 mAH , which is high when compared to about 12 mAH of that of polycrystalline electrolyte cell. Thus the cell capacity increases by about 4 mAH , when amorphous electrolytes are used in micropower sources.

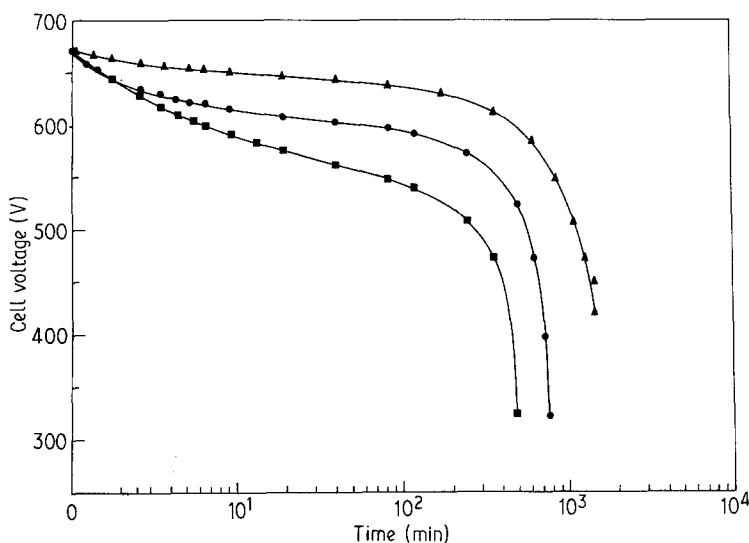


Figure 16 Illustration of the load characteristic curves for the amorphous electrolyte cells with \bullet corresponding to $\text{AgI-Ag}_2\text{O-V}_2\text{O}_5$, \blacksquare corresponding to $\text{AgI-Ag}_2\text{O-P}_2\text{O}_5$ and \blacktriangle corresponding to $\text{AgI-Ag}_2\text{O-V}_2\text{O}_5\text{-P}_2\text{O}_5$ systems respectively.

Acknowledgements

One of the authors (PSSNP) wishes to thank Professor C. A. Hogarth for interesting and inspiring discussions, Miss A. N. Durga Rani, who helped in the experimental work and Mr Anand for the dielectric data.

References

1. W. H. ZACHARIASEN, *J. Amer. Ceram. Soc.* **54** (1932) 3841.
2. T. MINAMI, K. IMAZAWA and M. TANAKA, *J. Non-Cryst. Solids* **42** (1980) 469.
3. P. SATHYA SAINATH PRASAD and S. RADHAKRISHNA, *Solid State Ionics* (1988) in press.
4. *Idem.*, *J. Non-Cryst. Solids* (1988) in press.
5. T. MINAMI, T. TAKUMA and M. TANAKA, *J. Electrochem. Soc.* **124** (1977) 1659.
6. K. HARIHARAN, R. KAUSHIK and S. RADHAKRISHNA, "Materials for Solids State Batteries", (World Scientific, Singapore, 1986) p. 325.
7. P. SATHYA SAINATH PRASAD and S. RADHAKRISHNA, *J. Mater. Sci. Lett.* **7** (1988) 113.
8. J. R. van WAZER, "Phosphorous and its Compounds", Vol. I (Interscience, New York, 1958) p. 733.
9. K. SHAHI and S. CHANDRA, *J. Phys. C.* **9** (1976) 3105.
10. *Idem.*, *Phys. Status Solidi a* **28** (1975) 653.
11. A. K. IVANOV-SHITS and V. S. BOROKOV, *Electrokhimiya* **16** (1980) 985.
12. H. B. GON and K. V. RAO, *Ind. J. Phys.* **54A** (1980) 50.

*Received 8 December 1987
and accepted 29 April 1988*